Atomic Spectroscopy

Article

Micro-area Quantitative and Imaging Analysis of the Qin Terracotta Warriors via Laser Ablation Inductively Coupled Plasma Mass Spectrometry

Guoxia Zhang, [a] Xiaoxi Li, [c] Desheng Lan, [c] Yin Xia, [c] Ping Zhou, [c] Qing Li, [a] and Zheng Wang [a,b,*]

[a] State Key Laboratory of High Performance Ceramics, Shanghai Institute of Ceramics, Chinese Academy of Sciences, Shanghai 201899, P. R. China

[b] Center of Materials Science and Optoelectronics Engineering, University of Chinese Academy of Sciences, Beijing 100049, P. R. China

[c] Emperor Qinshihuang's Mausoleum Site Museum, Xian, 710600, P. R. China

Received: *September 25, 2025;* ***Revised:*** *December 13, 2025;* ***Accepted:*** *December 13, 2025;* ***Available online:*** *December 13, 2025.*

DOI: 10.46770/AS.2025.157

ABSTRACT: The Terracotta Warriors, one of the most remarkable archaeological discoveries of the 20th century, provide critical insights into the artistic, technological, and military achievements of the Qin Dynasty. This study established a micro-area quantitative and imaging analysis method for the Qin Terracotta Warriors using laser ablation inductively coupled plasma mass spectrometry (LA-ICP-MS). Matrix-matched calibration standards were produced using the powder–pellet method, thereby ensuring the reliable quantification of both major and trace elements. Optimized ablation parameters (energy density of 8.3 J cm^{-2}, repetition rate of 20 Hz, and spot size of 100 μm) yielded stable signal intensities with relative standard deviations below 10%. The application of this method to multiple fragments of the Terracotta Warriors revealed compositional variations associated with color differences, structural layering, and excavation contexts. Quantitative accuracy ranged from 80% to 120%, and elemental imaging was achieved at a spatial resolution of 100 μm. High-resolution multielement maps illustrated the heterogeneous distributions of Cu, As, and Co linked to the pigment residues, offering new insights into pigment preparation techniques and post-burial alteration processes. Overall, the results demonstrate that LA-ICP-MS is a minimally destructive and high-resolution analytical tool that is well suited for the compositional and technological investigation of archaeological ceramics.

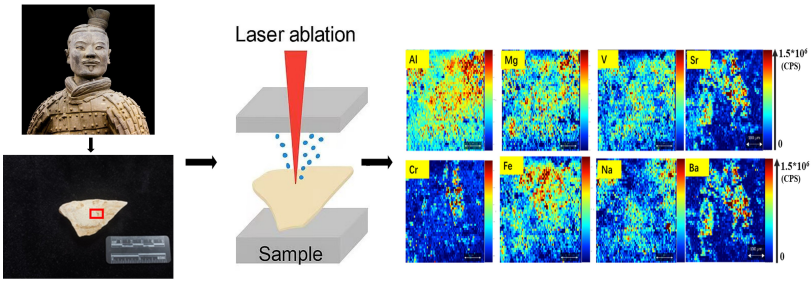

INTRODUCTION

By examining cultural artifacts, we can gain insights into historical social conditions, cultural achievements, and material civilization, thereby enhancing our appreciation of the richness and diversity of national cultures. Cultural relics serve as tangible evidence of past lifestyles and belief systems. Each artifact reflects the living habits, religious beliefs, and artistic expressions of its time, which makes them crucial resource for studying human civilization. Research on cultural relics helps us to recognize the value of cultural heritage and provides a scientific basis for their protection, restoration, and transmission.[1] Such studies enable us to better preserve and pass on these precious cultural legacies, allowing future generations to continue appreciating and learning from them.

The Terracotta Warriors, discovered in the Mausoleum of the First Qin Emperor, represent one of the most significant archaeological findings of the 20th century. These life-sized clay sculptures that date back over 2,000 years provide valuable insights into the artistic, technological, and military aspects of the Qin Dynasty.[2-3] However, because of prolonged burial, the

surfaces of the Terracotta Warriors have undergone various chemical and physical alterations. Hence, understanding the elemental composition of these artifacts is crucial for identifying raw material sources, reconstructing production processes, elucidating degradation mechanisms, and guiding restoration strategies. [4-8] The chemical fingerprinting of elements in cultural relics, particularly certain trace elements, enables the determination of their provenance, characteristics of the raw materials used, and potential manufacturing processes.[9] However, most minor and trace elements are not homogeneously distributed in the clay bodies.[10] Therefore, the trace element contents and their distribution in the pottery matrix are of great importance in the study of cultural relics. In summary, the elemental concentrations and distributions are indispensable aspects of research on the Terracotta Warriors. They are key to understanding the age, production techniques, and material origins of the artifacts; are critical for their preservation and restoration; and are also valuable for interpreting the cultural and symbolic meanings embedded in the artifacts. Conventional elemental analyses of cultural relics commonly employ techniques such as X-ray fluorescence spectroscopy (XRF) and energy-dispersive X-ray spectroscopy (EDS).[11-13] Researchers often use techniques such as XRF and scanning electron microscopy (SEM) to perform qualitative and quantitative analyses of the chemical elements in terracotta figurines, respectively. For example, Kurosawa and co-workers [5] applied optical microscopy (OM), petrographic microscopy (PM), scanning electron microscopy coupled with energy dispersive X-ray spectroscopy (SEM-EDS), and X-ray diffraction (XRD) to analyze several pottery sherds from the Svilengrad-Brantiite site in Bulgaria. X-ray diffraction (XRD) was used to identify mineral phases in terracotta artifacts, aiding in the determination of raw material sources and production technologies.[14] Although these techniques are useful for macroscopic or surface analyses, they generally offer limited sensitivity and are typically restricted to major elements. Moreover, their detectable element range is narrow, especially for low-atomic-number elements such as lithium, boron, and carbon, which cannot be detected using XRF.[15]

Elemental analysis at the micro-area level has become increasingly critical in archaeology because this method allows the spatially resolved characterization of pigments and substrates. Laser ablation inductively coupled plasma mass spectrometry (LA-ICP-MS) is a powerful analytical technique that enables micro-area and high-sensitivity elemental analysis without extensive sample preparation. This method allows both quantitative analysis and imaging of the spatial distribution of elements within samples.[16-21] In recent years, LA-ICP-MS has been widely applied in archaeological research to examine ceramics, pigments, and other cultural relics,[22-25] providing valuable trace-element data that can reveal information about the origin, manufacturing process, and post-burial alterations of artifacts. [26,27]

Research on the elemental analysis of archaeological ceramics using LA-ICP-MS has recently advanced significantly. Tite and Speakman and Neff applied LA-ICP-MS to provenance studies and technological assessments of ancient pottery, tracing raw material sources and manufacturing methods.[28,29] In China, research has mainly focused on the elemental analysis of the Terracotta Warriors and surrounding soil to identify the raw materials used in their creation.[30,31] Some studies have integrated LA-ICP-MS with other analytical techniques, such as XRF and SEM-EDS, to obtain more comprehensive compositional data.[32] Nevertheless, further investigation is needed into the micro-area distribution of elements across different structural layers of the Terracotta Warriors as well as the correlation between color variations and elemental composition.

This study aimed to develop and apply a micro-area quantitative and imaging analysis method using LA-ICP-MS to investigate the elemental composition of the Qin Terracotta Warriors. However, the accurate quantitative analysis of solid samples using LA-ICP-MS remains challenging, primarily because of uncertainties in the ablated sample quantity introduced by the laser system. These uncertainties lead to matrix effects and elemental fractionation, which can impact mass spectrometric signals.[33] Numerous studies have applied LA-ICP-MS to ceramics, soils, and ancient pigments. [34-36] The achievable analytical accuracy has often varied, with reported deviations of 5–20% for major elements and even larger discrepancies for trace elements when using silicate glasses as external calibrants. Moreover, achieving true micro-area quantification remains difficult because most available reference materials are not specifically designed to match the mineralogical and textural characteristics of archaeological ceramics. However, few reports have addressed matrix-matched standard preparation for Terracotta Warrior-type materials, nor have they provided a comprehensive validation of analytical accuracy and imaging resolution. This study aimed to fill this gap by establishing a reliable quantitative and imaging method using custom-prepared standards. Specifically, this study prepared matrix-matched reference materials that matched the ceramic relics. Quantitative analysis of major and trace elements was performed on fragments from various parts of the Terracotta Army during the same period. Finally, micro-area elemental imaging was performed on the relic surfaces to investigate the correlations between elemental distribution and surface color changes.

EXPERIMENTAL

Instrumentation. A laser ablation (LA) system (LSX-213, Newave, USA) was coupled to an ICP-MS instrument (ICAP-RQ, Thermo Fisher, USA) for LA-ICP-MS analysis. The digested samples were quantified using ICP-optical emission spectroscopy (ICP-OES) (5100, Agilent, USA). All dilutions were prepared

using high purity deionized water (18.25 MΩ·cm) obtained from a Milli-Q system (Millipore, Bedford, MA, USA). The operating conditions for the ICP-MS and laser ablation systems were optimized prior to analysis.

Reagents and Materials. All the samples were obtained from The Museum of the Terracotta Army of the Emperor Qin Shi Huang. After analysis, the ablation depth (<10 μm) and affected area (<200 μm × 1000 μm) showed no visible physical alteration or measurable change in chemical composition, as confirmed by optical microscopy. and was returned to continue the research on cultural relics, which will not affect subsequent restoration of the artifacts. Standard reference materials, including NIST glasses (NIST 610–616, National Institute of Standards and Technology, USA) and Chinese certified reference materials (GBW07405, GBW07407, GBW07449, GBW07455, and GBW07456; National Institute of Metrology, China), were used as matrix materials for preparing the lab-made reference materials. Liquid calibration standards were prepared from multielement standards of 100 mg/L (CCS-1, CCS-2, CCS-4, CCS-5, and CCS-6, Inorganic Ventures, USA). All solution-based calibrations were performed using 2 vol% HNO_3. Ultra-pure HF, HCl, $HCLO_4$ and HNO_3 (GR; Shanghai Aoban Technology Co., Ltd., Shanghai, China) were used for standard dissolution.

Parameters optimization for LA-ICP-MS analysis. Laser ablation (LA) is a physical process involving the breakdown of a solid into vapor and fine particulate matter. The interaction between the laser radiation and solid material is complex and depends on various laser parameters as well as the physical properties of the gas involved in the ablation. Previous studies indicated that optimizing these parameters and selecting appropriate purge gases can mitigate elemental fractionation. In this study, the laser parameters were optimized by monitoring the stability and repeatability of mass spectrometry signals. Optimization of the laser fluence, repetition rate, and carrier gas flow (He + Ar) was performed by monitoring the signal stability and minimizing fractionation. The optimized parameters were: an energy density of 8.3 J cm^{-2}, a repetition rate of 20 Hz, a spot size of 100 μm, a scan speed of 10 μm s^{-1}, and a carrier gas flow (He) of 0.7 L min^{-1}. The signal stability exceeded 90% over 60 s and the relative standard deviation (RSD) remained below 10%. By fine-tuning the laser settings and gas flow rates, elemental fractionation was minimized, thereby improving analytical accuracy and precision. Based on the direct solid sampling analysis technique, the introduction of interfering elements (*e.g.*, Cl and N) was avoided, which reduced the occurrence of mass spectral interference. In addition, elements such As, Se, Cr, and Ca were analyzed using the kinetic energy discrimination (KED) mode to eliminate interference during the experiment. The ablation points were carefully selected under an optical microscope to avoid cracks, weathered surfaces, and visible inclusions, while ensuring coverage of the typical and homogeneous matrix regions of each sample. For heterogeneous fragments, spots were evenly distributed across different micro-areas to account for possible compositional variations.

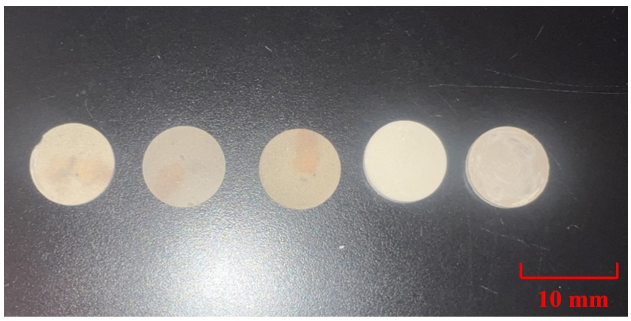

Fig. 1 An image of matrix-matched calibration standards.

Preparation of matrix-matched calibration standards. Matrix-matched solid standards were prepared based on terracotta figurines to ensure compatibility between the standard reference materials and samples. Based on the elemental content range in the terracotta figurines and the concentration gradient requirements for curve plotting, standard substances (GBW07405, GBW07407, GBW07449, GBW07455, and GBW07456) were selected, and doping concentrations were designed. For samples containing target elements, pellets were prepared by mixing 2.0 g of powdered reference material (GBW07405, GBW07407, GBW07449, GBW07455, or GBW07456 powder) with 0 mL, 1 mL, 2 mL, 4 mL and 10 mL of a 100 mg·L^{-1} multielement aqueous standard solution, followed by the addition of 20 mL water to prepare them for Std1, Std2, Std3, Std4, and Std5 samples, respectively. The suspension was stirred for 10 min, allowed to stand overnight, and dried into homogenized mixed powder by heating at 100 °C for approximately 5 h. Approximately 1 g of the dried mixture was pressed into a 10 mm diameter pellet under a pressure of 15 MPa for 10 s. The pellets were then fired in a muffle furnace at 1000 °C for 24 h, and pellets (Fig. 1) from both procedures were stored separately in clean plastic bags prior to LA-ICP-MS analysis.

Acid digestion of matrix-matched calibration standards for ICP-OES/MS analysis. For sample solubilization, 0.1 g of powdered standard was accurately weighed into a platinum dish and treated with 10 mL of HF and 2 mL of $HClO_4$ at 100 °C for 10 h. The solution was then heated to 180 °C until complete evaporation. Subsequently, 5 mL HCl was added to the platinum dish, and the solution was transferred to a 100 mL volumetric flask, which was filled to the mark with high-purity deionized water. A reagent blank was used throughout the process to correct for the elemental background contribution from the vessel after acid soaking. The final solutions were analyzed by ICP-OES and ICP-MS. The components Be^{9}, Cd^{112}, Er^{167}, Eu^{152}, Dy^{162}, Lu^{175}, Se^{78}, Sm^{150}, and Yb^{173} in std-1 were analyzed by ICP-MS, whereas the

results for the remaining components with higher concentrations were obtained by ICP-OES, with their characteristic analytical wavelengths selected to avoid spectral overlap and ensure a linear response.

RESULTS AND DISCUSSION

Evaluation of the performance of matrix-matched calibration standards. The performance of the laboratory-prepared standard reference materials was evaluated by analyzing their homogeneity and assigned values. Homogeneity and stability were assessed by conducting line scanning on the self-prepared standards using LA-ICP-MS in the line ablation mode. The homogeneity and stability of the standard materials were determined by observing the variations in the elemental signals along the ablation line. The elemental isotopes and trend of the signal intensity over time (Fig. 2) were obtained under conditions identical to those used for sample ablation. The homogeneity of the laboratory-prepared standards was evaluated using line-scan profiles and replicate analyses. The transient signals over 40 s (from 20–60 s) were stable, and the RSDs were 9.6% for ^{27}Al, 4.9% for ^{140}Ce and in the range of 4.9% to 9.6% for the other 26 elements, confirming satisfactory within-pellet uniformity.

Subsequently, the final standard reference materials were subjected to wet digestion. Both ICP-OES and ICP-MS were employed for the analysis, resulting in accurate determination of elemental concentrations in the solid standard reference materials. To ensure the accuracy of the quantitative curve constructed using matrix-matched calibration standards and the reliability of the quantitative analysis results, the elemental contents of the self-prepared reference materials are also critical. The theoretical addition amounts of the Std1, Std2, Std3, Std4, and Std5 samples were 0, 50, 100, 200, and 500 mg·kg^{-1}, respectively. To obtain accurate elemental concentrations, this study employed acid digestion combined with ICP-OES/MS to quantitatively analyze Std1, Std2, Std3, Std4, and Std5. The precise elemental contents of the self-prepared series of reference materials are presented in Table S1. The values shown in Table S1-a were determined using ICP-OES/MS after acid dissolution, and Table S1-b shows the reference values of the standard reference materials GBW07405, GBW07407, GBW07449, GBW07455, and GBW07456. The results demonstrated that the measured elemental concentrations in the laboratory-prepared reference materials were in close agreement with the theoretical doped values, indicating that the preparation method for the reference materials was contamination-free and exhibited high stability and reliability.

Calibration. Calibration remains challenging in LA analysis. LA-ICP-MS relies on the use of solid standards. However, accurate calibration curves can be negatively affected by fractionation and

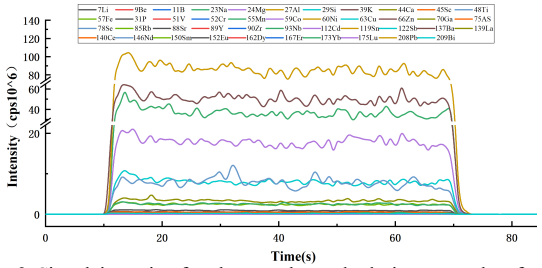

Fig. 2 Signal intensity for the metal standards in a sample of matrix-matched calibrant as a function of ablation time during LA-ICP-MS.

matrix effects. LA-ICP-MS was used to sequentially ablate a series of self-prepared standard materials and measure the signal intensities of the elements. Calibration curves were conventionally obtained through linear least-squares regression of the integrated ion signal (y-axis) against the amount of analyte added (x-axis) to the sample divided by the area. The curves exhibited excellent linearity, allowing quantification of major elements, minor elements, and trace elements in real samples. The relationship coefficients calculated for all 28 elements range from 0.99 to 0.9999. This high degree of correlation strongly indicates that both the standard sample preparation procedure and the employed data collection and processing strategies were highly appropriate and reliable for the intended analysis.

Quantitative analysis and method validation of major and minor elements in fragments of Qin Terracotta Warriors with different colors. In this study, LA-ICP-MS was employed to conduct comprehensive elemental analyses of self-prepared standard materials labeled SX-XA-QY-1 through SX-XA-QY-7, representing fragments of the Qin Terracotta Warriors of various colors. Detailed sample information is provided in Table S2, "Qin Terracotta Warrior Ceramic Fragments Samples." Using the experimental standard curves obtained, quantitative analyses of the major and minor elements in the differently colored fragments were performed.

A total of 26 elements were detected, including major elements (Na, Mg, Al, Si, K, Ca, Ti, and Fe) and minor-to-trace elements (P, Sc, V, Cr, Mn, Co, Ni, Cu, Zn, Rb, Sr, Zr, Ba, La, Ce, Nd, Lu, and Pb). The quantitative results for the major elements are presented in Table S3-a, while those for the minor and trace elements are listed in Table S3-b. Analysis of these tables revealed that the color variations and elemental compositions of the Qin Terracotta Warrior fragments differed, correlating the observed color differences with specific elemental signatures. The data indicate that the concentrations of elements such as Fe, Mn, and Cr vary considerably across pottery fragments of different colors. However, the specific contribution of any single element to the coloration of the Terracotta Warriors cannot be determined definitively. Although the coloration of the pottery figurines is strongly influenced by elemental content, additional factors,

including oxidation states (*e.g.*, Fe^{2+} vs. Fe^{3+}) and the proportional relationships among chromophoric elements also govern the coloration. These findings highlight the intricate nature of the pigment systems in Qin-era ceramics.

To verify the accuracy of the analytical method, comparative analyses were conducted on the SX-XA-QL-3 and SX-XA-QL-5 samples. XRF was employed, and the results are presented in Table S4. These data indicate that XRF effectively detects high-concentration elements; however, this technique is less sensitive to low-concentration elements, leading to the potential omission of trace element information. A comparison of the quantitative results for high-concentration elements obtained through XRF and the primary method revealed strong consistency, further confirming the accuracy and reliability of the established analytical approach.

Quantitative analysis of major and minor elements in fragments of Qin Terracotta Warriors from different parts. The elemental compositions of the fragmented remains from different parts of the Terracotta Warriors may vary primarily because of differences in raw materials, pigment formulations, and manufacturing techniques. The Terracotta Warriors were generally made of fine clay and coated with layers of polychrome paint containing various mineral elements such as Cu, Pb, Fe, Mn, and As. Depending on the preservation conditions of each part, the residual pigments on the surface and their chemical interactions with the burial environment may have led to variations in elemental composition across different sections. Furthermore, by comparing the characteristic elemental profiles of various body parts, differences in the production processes, firing temperatures, and even the workshop origins of the statues may be inferred.

Using LA-ICP-MS in conjunction with the matrix-matched calibration method described above, quantitative analyses were conducted on Terracotta Warrior samples from distinct body parts, including fragments from the cuff (G8-21), robe (G8-22), and armor (G8-25), as well as surface coatings, inner linings, armor plates, and bottom robe sections, which total 18 representative specimens (Table S5). The obtained results (Tables S6-a and S6-b) provide comprehensive datasets of major and trace element concentrations for both the surface and subsurface layers.

Comparative analysis revealed clear compositional differences among the body parts. The armor fragments exhibited elevated Fe, Mn, and Co contents, consistent with the intentional application of black or dark pigments based on iron and manganese oxides. The robe and sleeve fragments contained relatively high Na, Al, and K concentrations, corresponding to aluminosilicate-rich clay matrices and lighter pigment residues. The waist and belt fragments were enriched in As and occasionally in Pb, suggesting the use of green-blue pigments derived from As or lead-based compounds. These inter-part differences suggest that distinct pigment recipes and raw materials were employed for the different components of the figures, possibly reflecting the functional or visual hierarchies in their original appearances. Moreover, the geochemical variability among the clay matrices supports the hypothesis that separate workshops or production batches contributed to different body parts, each sourcing local raw materials with characteristic elemental fingerprints.

Overall, the quantitative data obtained through LA-ICP-MS not only provide a detailed elemental inventory of the Terracotta Warrior fragments but also offer critical evidence for understanding technological diversity, regional material sourcing, and preservation techniques within the Qin terracotta production system.

Quantitative analysis of major and trace elements in Terracotta Warrior fragments from different excavation sites of the same period. The relationship between major and trace elements and the origin of the Terracotta Warriors is a nuanced archaeological and scientific problem that primarily relies on modern technological methods to analyze the elemental composition of both the Terracotta Warriors and surrounding soils. The sources of raw materials and kiln locations for the creation of the Terracotta Army have long been a focal point of interest for archaeologists and enthusiasts alike. To address these questions, researchers have employed various modern scientific methods, with the analysis of major and trace elements serving as crucial tools for revealing the provenance of the Terracotta Warriors. Trace elements play a key role in identifying the origins of the Terracotta Warriors. Owing to variations in soil and mineral compositions across different regions, these differences are reflected in the elemental composition of artifacts such as the Terracotta Warriors. Therefore, by comparing the trace element contents and characteristics of the Terracotta Warriors and surrounding soil samples, researchers can infer the sources of the materials used.

In this study, LA-ICP-MS was employed to measure the concentrations of major and trace elements in each sample, particularly trace elements that are not influenced by human control or manufacturing processes, such as Ba, Mn, and Co. Subsequently, using lab-made solid reference materials, a quantitative analysis of major and trace elements in fragments of the Terracotta Warriors from different excavation sites during the same period (Fig. 3) was performed, and the results are presented

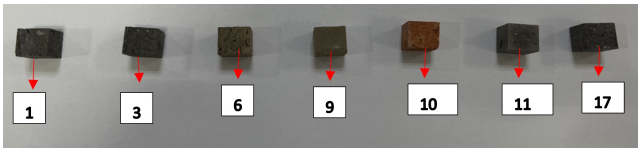

Fig. 3 Terracotta Warrior Samples from Different Excavation Sites of the Same Period.

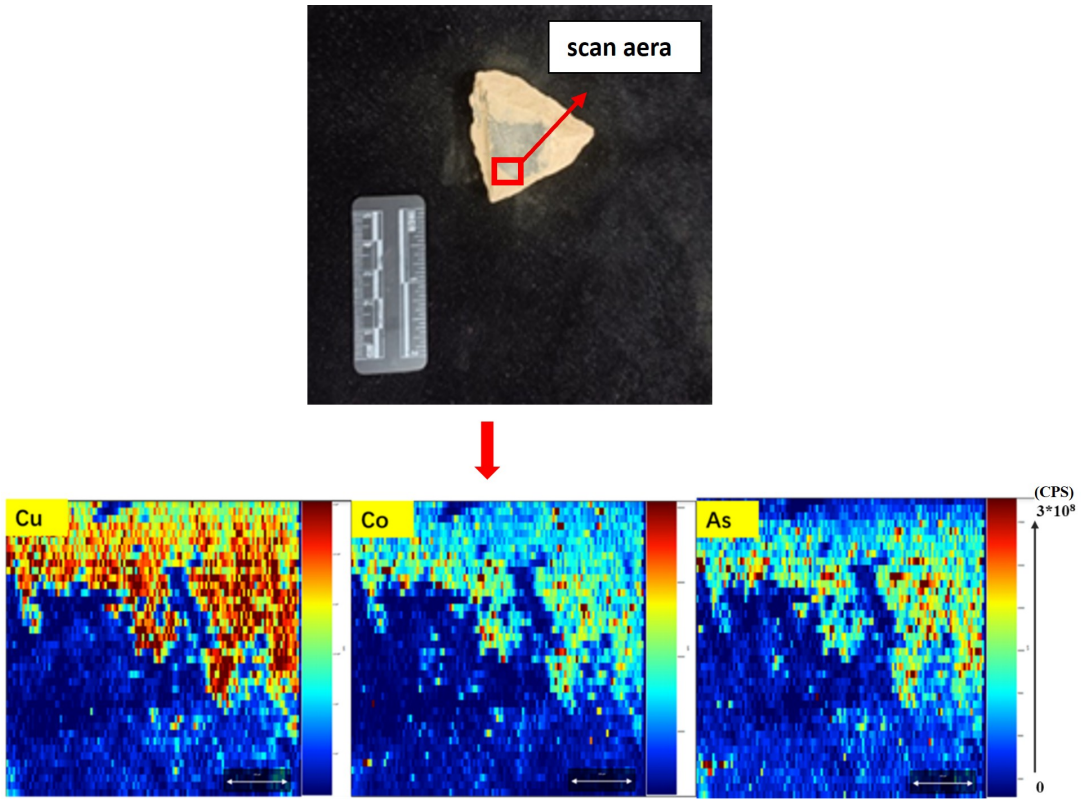

Fig. 4 Image of an armor fragment sample and distribution images of Cu, Co, and As by LA-ICP-MS mapping.

in Tables S7-a and S7-b. As shown in the Table S7, significant differences exist in the elemental composition of the pottery fragments excavated from different sites during the same period. Due to the limited number of samples available in this study, identifying "fingerprint elements" and constructing a data model for provenance discrimination remains challenging. Nonetheless, this study demonstrates that LA-ICP-MS is a versatile technique for trace-element analysis of pottery fragments, offering methodological insights and guiding future research directions.

Elemental distribution and imaging analysis of the Terracotta Warrior fragments. The LA-ICP-MS technique not only enables quantitative elemental analysis, but also provides powerful capabilities for micro-area elemental imaging. In this study, surface line and area scans were performed on selected regions of Terracotta Warrior fragments with different surface colors. By integrating the ablation signal intensities across the scanned areas, multielement distribution maps were generated, allowing direct visualization of the spatial correlations between the elemental concentrations and pigment colors. Regions of interest (ROIs) were carefully selected according to visible color variations to ensure representative elemental mapping. Specifically, samples from the inner side of the robe, which exhibited uneven color tones, and armor fragments with black surface coatings were analyzed in detail. The red-marked areas in Figs. 4 and 5 indicate the laser ablation tracks where the elemental signals were collected.

The resulting multielement maps clearly demonstrate that the color heterogeneity of the inner robe fragments is associated with variations in Na, Mg, Al, V, Cr, Fe, Ga, Rb, Sr, Sb, Cs, and Ba. In contrast, elements such as Cu, As, and Co were highly enriched in dark- or black-colored areas, corresponding to pigment residues, whereas Mn and Fe displayed more uniform distributions within the ceramic matrix. These visualized correlations between elemental enrichment and color provide direct evidence of intentional pigment application as well as post-burial oxidation of iron-bearing minerals. Overall, the multielement imaging results offer valuable insights into the pigment composition and preservation state, supporting future restoration and color reconstruction studies of the Terracotta Warriors.

The detection limits of the 28 elements analyzed in this study ranged from 0.5 to 50 $mg \cdot kg^{-1}$, calculated following the conventional 3σ criterion. Specifically, the LOD for each element was determined as three times the standard deviation of ten replicate measurements of the blank (or background signal) divided by the slope of the corresponding calibration curve. This procedure ensures that instrumental noise, baseline drift, and calibration sensitivity are consistently accounted for in analytical detection.

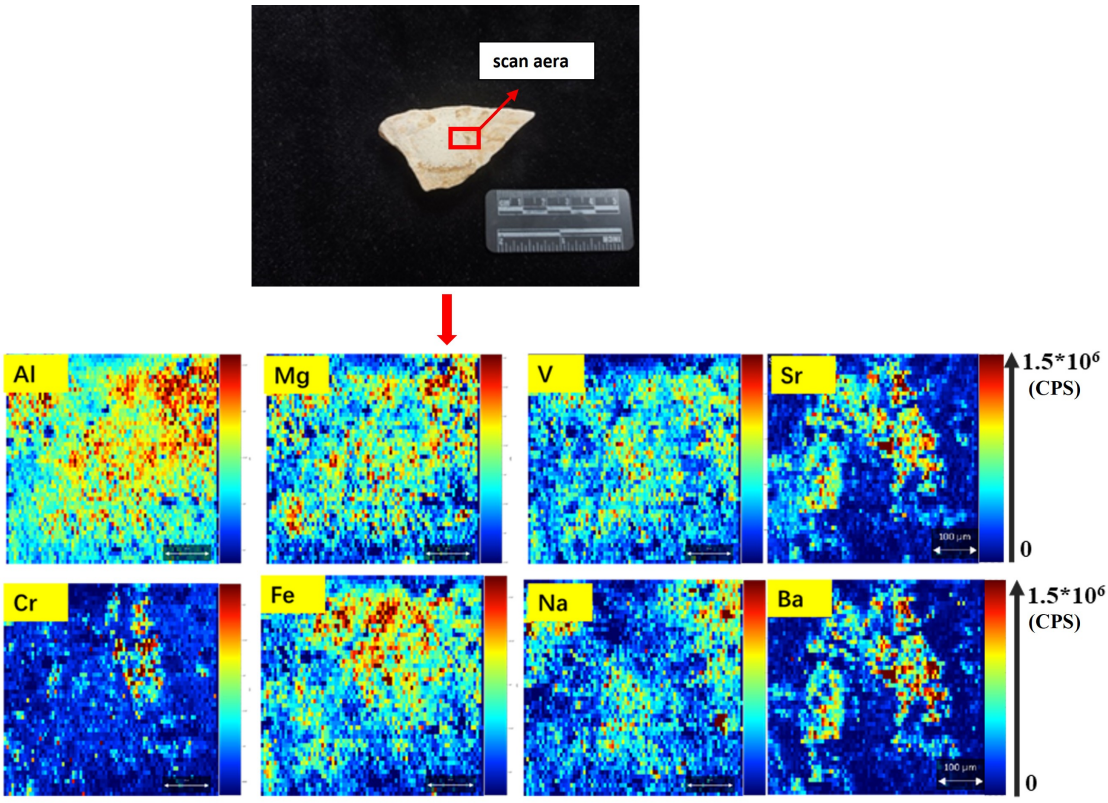

Fig. 5 Image of the inner side of a robe sample and distribution images of Al, Mg, V, Sr, Cr, Fe, Na, and Ba by LA-ICP-MS mapping.

CONCLUSION

In this study, LA-ICP-MS was successfully applied to perform micro-area quantitative and imaging analysis of the Qin Terracotta Warriors. By optimizing the laser ablation parameters and preparing matrix-matched standard reference materials, high-precision quantitative analysis of the major and trace elements was achieved. The results provide valuable insights into the elemental compositions of different fragments, revealing variations associated with color, structural layers, and excavation sites. These findings contribute to a deeper understanding of the raw material sources, manufacturing techniques, and post-burial alterations of the artifacts.

Furthermore, elemental imaging analysis enabled the visualization of spatial element distributions, shedding light on pigment degradation and surface alterations. The correlation between elemental composition and surface color provides important clues for studying the changes over the years in the appearance of the Terracotta Warriors. This study also demonstrated that LA-ICP-MS is a powerful tool for minimally destructive elemental analysis, offering a more comprehensive approach to cultural heritage research. Overall, this study enhances our understanding of the composition and preservation of the Qin Terracotta Warriors, providing a scientific basis for their restoration and long-term conservation. The methodological advancements in this study can also be applied to the analysis of other archaeological ceramics, contributing to broader efforts in cultural heritage protection and material characterization.

ASSOCIATED CONTENT

The supporting information (Tables S1–S7) is available at https://www.at-spectrosc.com.

AUTHOR INFORMATION

Zheng Wang received his PhD in 2006 from the Shanghai Institute of Ceramics, Chinese Academy of Sciences (CAS). He is a research professor and PhD supervisor at the Shanghai Institute of Ceramics, CAS. His major research interests are environmental analytical chemistry, spectroscopy instrument development, preparation and characterization of new inorganic materials, 3D printing materials and precision manufacturing, etc. He has been working as member of editorial board for *Atomic Spectroscopy*,

Chinese Chemical Letters, and *Spectroscopy and Spectral Analysis*. Zheng Wang is author or co-author of over 100 articles published in peer-reviewed scientific journals. In 2010 and 2018, he received two science and technology awards from the China Association for Analysis and Testing.

Corresponding Author

*Z. Wang

Email address: wangzheng@mail.sic.ac.cn

Notes

The authors declare no competing financial interest.

ACKNOWLEDGMENTS

This work was supported by the Key Research and Development Program of Shaanxi (2022LL-ZD-01), Youth Open Research Project of the Emperor Qinshihuang's Mausoleum Site Museum (QKFKT202113), the National Natural Science Foundation of China (12105354), the Shanghai Technical Platform for Testing and Characterization on Inorganic Materials (19DZ2290700).

REFERENCES

1. Y. Xiong, *China Ceramics*, 2006, **42**, 56-57. https://d.wanfangdata.com.cn/periodical/zgtc200612020
2. J. X Liang, T. Wang, Y. X. Zhang, F. Wang, Q. Li, H. J. Luo, X. C. Zhao, and J. F. Zhu, *Spectrosc. Spectr. Anal.*, 2023, **43**, 175-182. https://doi.org/10.3964/j.issn.1000-0593(2023)01-0175-08
3. G. X. Li, W. J. Zhao, R. W. Li, Z. Y. Gao, J.Z. Xie, G. H. Han, S. L. Feng, D. Y. Fan, Y. Zhang, Z. F. Chai, Z. L. Zhang, and J. X. Zhu, *Nucl. Phys. Rev.*, 2002, **19**, 416-420. https://doi.org/10.11804/NuclPhysRev.19.04.416
4. P. Quinn, Y. Yang, Y. Xia, X. Li, S. Ma, S. Zhang, and D. Wilke, *Archaeometry*, 2021, **63**, 40–52. https://doi.org/10.1111/arcm.12613
5. M. Kurosawa, M Semmoto, and T. Shibata, *Minerals*, 2022, **12**, 1-18. https://doi.org/10.3390/min12010079
6. R. Mentesana, A. Hein, M. M. Fernàndez, V. Kilikoglou, and J. B. Garrigós, *Minerals*, 2022, **12**, 35-72. https://doi.org/10.3390/min12040423
7. Z. Xu, *Mediterr. Archaeol. AR.*, 2024, **24**, 191–205. https://www.maajournal.com/index.php/maa/article/view/1302
8. I. Coutinho, I. C. Campaña, L. C. Alves, and T. Medici, *Minerals*, 2021, **11**, 149-168. https://doi.org/10.3390/min11070688
9. D. Braekmans, V. Boschloos, H. Hameeuw, and A. Van der Perre, *Microchem. J.*, 2019, **145**, 1207-1217. https://doi.org/10.1016/j.microc.2018.12.029
10. G. Rapp, and C. L. Hill, Geoarchaeology: The Earth-Science Approach to Archaeological Interpretation, Yale University Press, London, 2006. https://www.jstor.org/stable/j.ctt1cc2kd9
11. Y. C. Liu, Q. Ji, X. R. Wang, J. Yang, J. K. O'Connor, B. Guo, T. L. Ren, T. T. Yin, and Y. B. Wang, *Atom. Spectrosc.*, 2024, **45**, 123-131. https://doi.org/10.46770/AS.2024.033
12. J. Emmitt, A. McAlister, and J. Armstrong, *Minerals*, 2021, **11**, 113-132. https://doi.org/10.3390/min 11070697
13. T. J. Gao, and W. B. Hsu, *Atom. Spectrosc*., 2025, **46**, 221-229. https://doi.org/10.46770/AS.2025.013
14. S. Solongo, S. Tengis, G. Enkhbat, B. Orgil, and L. M. Erdenebold, *Archaeometry*, 2023, **65**, 49–63. https://doi.org/10.1111/arcm.12799
15. C. Fabre, D. Devismes, S. Moncayo, F. Pelascini, F. Trichard, A. Lecomte, B. Bousquet, J. Cauzid, and V. Motto-Ros, *J. Anal. At. Spectrom.*, 2018, **33**, 1345–1353. https://doi.org/10.1039/c8ja00048d
16. Y. S. Liu, Z. C. Hu, S. Gao, D. Günther, J. Xu, H. G Gao, and H. H. Chen, *Chem. Geol.*, 2008, **257**, 34-43. https://doi.org/10.1016/j.chemgeo.2008.08.004
17. Y. Wang, Y.J Wei, Y. Lu, J. Wang, X. S. Wang, Z. Shao, M. L. Chen, and J. H. Wang, *Atom. Spectrosc.*, 2023, **44**, 401-408. https://doi.org/10.46770/AS.2023.280
18. N. S. Medvedev, V. D. Kurbatova, T. Y. Guselnikova, and A. I. Saprykin, *Atom. Spectrosc.*, 2024, **45**, 26-32. https://doi.org/10.46770/AS.2023.256
19. H. L. Li, J. Z. Zhou, W. Guo, and S. H. Hu, *Atom. Spectrosc.*, 2025, **46**, 297-304. https://doi.org/10.46770/AS.2025.081
20. G. C. Sun, M. Y. Chen, J. J. Huo, Y. G. Li, R. X Chen, G. Q. Liu, L. Q. Dai, Z. F. Zhao, H.O. Gu, P. Gao, and S. B. Zhang, *Atom. Spectrosc.*, 2025, **46**, 185-197. https://doi.org/10.46770/AS.2025.012
21. D. Chew, K. Drost, J. H. Marsh, and J. A. Petrus, *Chem. Geol.*, 2021, **559**, 119917. https://doi.org/10.1016/j.chemgeo.2020.119917
22. P. J. Sylvester, and S. E. Jackson, *Elements*, 2016, **12**, 307–310. https://doi.org/10.2113/gselements.12.5.307
23. B. W. Wang, Q. W. L. Zhang, J. W. Delano, D. Zhang, D. J. Ouyang, M. H. Yang, S. T. Wu, and Q. L. Li, *Atom. Spectrosc.*, 2025, **46**, 119-130. https://doi.org/10.46770/AS.2025.055
24. M. Burger, A. G. Graham, S. Allner, G. Schwarz, H. A. O. Wang, L. Gyr, S. Burgener, B. Hattendorf, D. Grolimund, and D. Günther, *Anal. Chem.*, 2015, **87**, 8259–8267. https://doi.org/10.1021/acs.analchem.5b01977
25. G. Craig, M. S. A. Horstwood, H. J. Reid, and B. L. Sharp, *J. Anal. At. Spectrom.*, 2020, **35**, 1011–1021. https://doi.org/10.1039/d0ja00066c
26. K. Drost, D. Chew, J. A. Petrus, F. Scholze, J. D. Woodhead, J. W. Schneider, and D. A. T. Harper, Geophys. Geosystems, 2018, **19**, 4631–4648. https://doi.org/10.1029/2018GC007850
27. S. M. Eggins, R. Grün, M. T. McCulloch, A. W. G. Pike, J. Chappell, L. Kinsley, G. Mortimer, M. Shelley, C. V. Murray-Wallace, C. Spötl, and L. Taylor, *Quat. Sci. Rev.*, 2005, **24**, 2523–2538. https://doi.org/10.1016/j.quascirev.2005.07.006
28. L. George, N.J. Cook, C. Cristiana, and B. P. Wade, *Am. Mineral.*, 2015, **100**, 548–569. https://doi.org/10.2138/am-2015-4862
29. D. Kaeter, R. Barros, J. F. Menuge, and D. M. Chew, *Geochim. Cosmochim. Acta*, 2018, **240**, 98–130. https://doi.org/10.1016/j.gca.2018.08.024
30. T. Raimondo, J. Payne, B. Wade, P. Lanari, C. Clark, and M. Hand, *Contrib. Mineral. Petrol.*, 2017, 172, 17. https://doi.org/10.1007/s00410-017-1339-z
31. R. J. Speakman1, M. D. Glascock, R. H. Tykot, C. Descantes, J. J. Thatcher, C. E. Skinner, and K. M. Lienhop, *Archaeological Chemistry*, 2007, **15**, 275-296. https://doi.org/10.1021/bk-2007-0968.ch015
32. K. P. Wright, E. H. Blair, I. Thompson, and L. Dussubieux, *J. Archaeol. Sci. Rep.*, 2024, **55**, 104468. https://doi.org/10.1016/j.jasrep.2024.104468

33. M. Guillong, and D. Günther, *J. Anal. At. Spectrom*., 2002,**17**, 831-837. https://doi.org/10.1039/B202988J

34 .W. Cui, Z. Cai, Q. Li, H. Y. Qu, J. Q. Zheng, D. G. Yu, J. F. Chen, and Z. Wang, Talanta, 2023, **255**, 124248. https://doi.org/10.1016/j.talanta.2022.124248

35. A. Lores-Padín, B. Fernández, M. García, H. González-Iglesias, and R. Pereiro, *Anal. Chim. Acta*, 2022, **1221**, 340128. https://doi.org/10.1016/j.aca.2022.340128

36. H. Pan, L. Feng, Y. Lu, Y. Han, J. Xiong, and H. Li, *TrAC-Trend. Anal. Chem.*, 2022, **156**, 116710. https://doi.org/10.1016/j.trac.2022.116710